CHAPTER 3 DENUDATION OF SOURCE TERRAINS

(With major contributions by Gregory E. Tucker)

The previous chapter presented some basic tectonophysical principles that affect sedimentary basins and source terrains. For simplicity, topographically high areas adjacent to basins were not allowed to erode, and a thickening fold and thrust belt, for example, was treated solely as a load that produced a flexural moat. In reality, a thrust belt is eroded and provides a source terrain for an adjacent foreland basin. Here, we rectify this shortcoming by including a simple source denudation model, which is necessary for two reasons. First, redistribution of mass by surface processes affects the mechanics of crustal thickening and crustal flexure. Forward propagation of thrusts, for example, is partly controlled by the rate at which material is unloaded from fault-bend folds at ramps, and the geometry of critically tapered accretionary wedges depends upon erosion of their upper surfaces. Second, the characteristics of the basin's fill depend upon the characteristics of sediment and the rate at which it is supplied to the basin, both being determined by the mechanics of source denudation.

The denudation of a source terrain and delivery of sediment to a basin is conceptualized in two steps that are interconnected in nature but separated here for clarity. The first involves denuding the source terrain, which involves delivery of sediment and water to a trunk stream from various drainage basins. It forms the topic of this chapter. The second, presented in Chapter 4, consists of conveying the sediment and water in the trunk stream to the basin.

Modeling denudation, or more precisely, modeling yields of water and sediment from drainage basins, is difficult because various geologic, climatic, and topographic settings need to be considered. After 50 years' effort, the procedures are still in infancy. Extant models range from multivariate regression equations based on data from river-gauging stations, to complicated models like the *Stanford Watershed Model*, which require 20 or 30 parameters to describe specific catchment characteristics such as infiltration indices, storage thresholds for

ground water, and soil depths. Consistent with our objectives, we steer an intermediate course, providing a first-order landscape evolution model to suggest how denudation might be treated, while also providing simple empirical functions of source denudation and water and sediment yields where a less complicated model is desired. However we do it, we need to predict the amount of load eroded from a source terrain during a timestep, and the amount of clastic sediment fed in turn to streams entering our model basin.

A LANDSCAPE DENUDATION MODEL

Creating a landscape denudation model involves identifying the essential processes that create landscapes, mathematically describing these processes, linking the mathematical descriptions together, and then forecasting the resulting landscape evolution with its constantly changing morphology and water and sediment discharges. The task may seem Herculean but is manageable if we take our cue from experimentalists in geomorphology who simplify their models by using homogenous disaggregated earth materials. The codes for any model always can be expanded later to include complications and more detail. Below we present what is arguably the simplest landscape model that still captures the basic landscape-forming processes. The model was developed by Greg Tucker while he was a graduate student at Penn State University and was fashioned after the pioneering works of Ahnert (1976) and Willgoose (Willgoose, Bras, and Rodriguez-Iturbe, 1991).

Identification of the essential processes in landscape development is helped by sandbox experiments that geomorphologists, such as Stan Shumm at Colorado State University, use to study the evolution of drainage nets. Shumm and students (Schumm, Mosley, and Weaver, 1987) used a 9 x 15-m box initially filled with a homogeneous mixture of plaster sand and floodplain sediment that sloped towards an outlet. An overhead sprinkler system provided a uniform distribution of precipitation. A typical experiment consisted of setting the baselevel at the outset, starting the sprinklers and maintaining them at a constant rate of application, and observing the evolving landscape. Such a model physically simulates rainsplash, sheetflow, concentrated runoff in channels, and mass movement, although it does not represent soil formation, variable erodibility, glacial erosion, tectonic uplift, or the effects of vegetation. We can try to capture all these processes in our numerical model, as well as consider tectonic uplift.

Physical Principles

Conservation of mass is the basic physical principle that serves as our starting point. A landscape can be represented by an N by M square grid of vertical columns of varying elevations as in Figure 3-1. Let each column define a cell and the height of each cell be $h(x,y)$. The principle of mass conservation states that:

$$\text{Time rate of change of mass in a cell} = \text{mass rate in} - \text{mass rate out} \qquad \textbf{(3-1)}$$

The mass in a cell is its density times its volume. Let each cell be of cross-sectional area dy by dx, such that its volume is $h\,dy\,dx$. Then the first term in (3-1) can be written:

$$\frac{\partial}{\partial t}\sigma h dy dx \qquad \textbf{(3-2)}$$

where: σ = bulk density of cell.

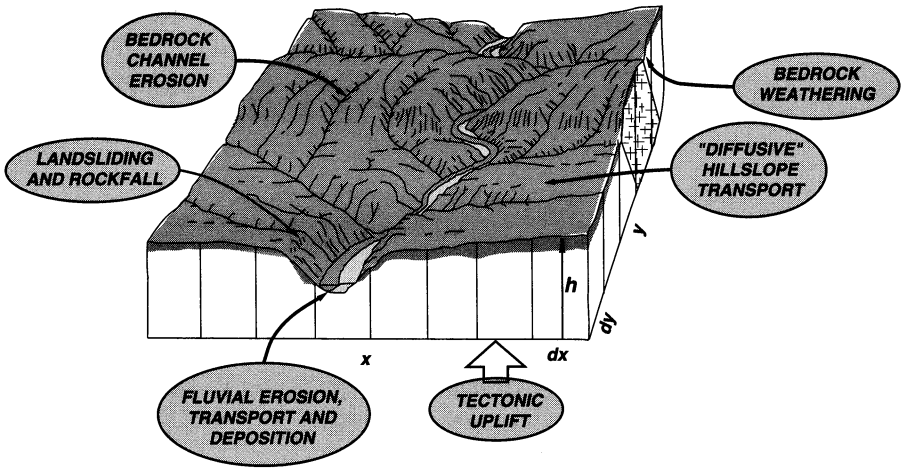

Figure 3-1 Grid and processes in landscape model.

What are the mass rates of earth materials (rocks, soil, sediment) into and out of cells? These are functions of the processes listed above: rainsplash, sheetflow, concentrated runoff in channels, mass movement, and tectonic thickening. Here we combine the mass transfer on hillslopes due to rainsplash, sheetflow, and mass movements such as rockfalls, avalanches, and soil creep, into one transfer function, which for the moment, we will call the hillslope function B. Think of $B(x,y,t)$ as the mass in kilograms of earth material passing from one cell to a neighbor per unit time per unit cell width. The mass transfer among cells of sediment and dissolved load in stream channels will be called $q_s(x,y,t)$, and it too has units of kg/s/m. Finally, let the rate of mass addition to each cell due to tectonic thickening be $R(x,y,t)$ in units of kg/s/m^2.

Because mass can enter each cell in both the x and y directions, it is convenient to consider each direction separately, starting with the x direction. The total mass entering a cell in the x direction per unit time due to mass movements will be $B_x dy$. What is the mass rate out of the cell at position $x + dx$? Remarkably, it can be defined in terms of the mass rate in at x, thanks to a theorem due to Brook Taylor, an early eighteenth century British mathematician. Taylor's *Methodus inrementorum directa et inversa (1715)* invented a new branch of higher mathematics, now called the calculus of finite differences, and contains the celebrated formula known as Taylor's theorem. Taylor's theorem states that if a function is analytic, and if its value is known at a point a, then the value of the function a differential distance ds away from a is:

$$f(a+ds) = \left[f(a) + \frac{\partial}{\partial s} f(a)ds + \ldots\right] \quad \textbf{(3-3)}$$

where the dots signify higher-order terms that become negligible as ds goes to zero.

Therefore, the mass rate out can be written as:

$$B_x + \frac{\partial B_x}{\partial x} dx \quad \textbf{(3-4)}$$

and therefore the right-hand side of (3-1) becomes:

$$B_x dy - (B_x + \frac{\partial B_x}{\partial x} dx)\, dy = -\frac{\partial B_x}{\partial x} dydx \qquad \textbf{(3-5)}$$

By analogy, the term for q_{sx} is:

$$-\frac{\partial q_{sx}}{\partial x} dydx \qquad \textbf{(3-6)}$$

The same logic applies in the y direction, such that the net mass flux entering a cell in that direction is:

$$-\frac{\partial B_y}{\partial y} dydx - \frac{\partial q_{sy}}{\partial y} dydx \qquad \textbf{(3-7)}$$

Substituting (3-2), (3-5), (3-6), (3-7), and the definition for tectonic thickening into (3-1), and clearing terms, yields:

$$\sigma \frac{\partial h}{\partial t} = -(\frac{\partial B_x}{\partial x} + \frac{\partial B_y}{\partial y}) - (\frac{\partial q_{sx}}{\partial x} + \frac{\partial q_{sy}}{\partial y}) + R \qquad \textbf{(3-8)}$$

This is the basic equation which must be solved for h as a function of x, y, and t. It contains the three functions, B, q_s, and R, which remain to be specified.

First, consider the hillslope function B. As noted above, it represents the rate at which sediment is transferred into and out of cells due to hillslope processes. Geomorphologists may agree that the long-term average mass flux of material on hillslopes can be modeled as a diffusion process where mass flux is proportional to slope:

$$B_x = -D_x \frac{\partial h}{\partial x} \qquad \textbf{(3-9)}$$

where: D_x = diffusion coefficient (units of kg $m^{-1}s^{-1}$) in x direction (negative sign ensures that mass flows downslope).

Next consider q_s, the function describing mass transfer in channels, consisting of the combined bedload and suspended load per unit width of channel. In subsequent chapters it will be derived from first principles. For the present purposes, it is defined after Willgoose (1989), with the immersed-weight sediment transport rate per unit flow width, i_b, proportional to the mean-available stream power per unit flow width:

$$i_b \propto \rho g q^m S^n \qquad \textbf{(3-10)}$$

where: ρ = density of the fluid,
g = gravitational acceleration,
q = water discharge per unit flow width,
S = the energy slope of the stream,
m and n = exponents.

Dividing by gravitational acceleration to obtain a mass transport rate, q_s, yields:

$$q_s = k\rho q^m S^n \tag{3-11}$$

where: k = dimensionless proportionality constant.

Substituting (3-9) and (3-11) into (3-8)yields:

$$\sigma\frac{\partial h}{\partial t} = \left[\frac{\partial}{\partial x}D_x\frac{\partial h}{\partial x} + \frac{\partial}{\partial y}D_y\frac{\partial h}{\partial y}\right] - k\rho\left[\frac{\partial}{\partial x}q_x^m S_x^n + \frac{\partial}{\partial y}q_y^m S_y^n\right] + R \tag{3-12}$$

Finally, consider R, the function describing mass flux into a cell due to tectonic thickening. It is related to the more conventional uplift rate U in m/s:

$$R = \sigma U \tag{3-13}$$

Note that if sediment transport in channels is set to zero and there is no tectonic uplift, (3-12) takes the form of a two-dimensional diffusion equation. It is completely analogous to the heat diffusion equation and can be solved by identical means. Conversely, if hillslope and tectonic processes are set to zero, and for simplicity considering only one horizontal dimension, (3-12) becomes:

$$\frac{\partial h}{\partial t} = -\frac{k\rho}{\sigma}\left(\frac{\partial}{\partial x}q_x S_x\right) \tag{3-14}$$

Solution of (3-12) by finite differences is accomplished in a FORTRAN program called GOLEM (Program 3), which stands for Geophysical Orogenic Landscape Evolution Model.

Model Description

Three primary modules have been constructed in GOLEM to simulate landscape development. First is a routing module that calculates the passage of water across the landscape. It assumes that any parcel of water entering the landscape via precipitation travels by overland flow down the steepest slope from cell to cell until it encounters a boundary cell. Within the routing module a submodule calculates the drainage of closed basins (lakes) and another submodule calculates the presence or absence of channel segments in each cell, based on a threshold function of discharge and slope. The second module deals with sediment transport and is broken into two submodules, one for calculating hillslope sediment transport, and the other for calculating fluvial sediment transport. Hillslope transport consists of the mass diffusion term in (3-12). It is solved using the alternating-direction implicit (ADI) method of Peaceman and Rachford (Smith, 1978). For a discussion of an implicit solution to the diffusion equation, see Chapter 5 on deltas. Fluvial sediment transport occurs only in cells that contain channels. GOLEM calculates sediment transport in channels by balancing a mass continuity equation for the channel bed, where available stream power at a cell governs the sediment flux rate out of that cell. Finally, GOLEM provides two different uplift modes, a spatially uniform uplift across the whole grid, and a fault block uplift simulated by rotation about a hingeline.

Descriptions of Routines in GOLEM

Because the model is moderately complicated, a brief description is offered here. The MAIN routine first calls the INITIALIZE subroutine. INITIALIZE reads model parameter values from a file called 'lem.in', as well as the names for the initial topography and output files. Once these data have been read in, INITIAL-

IZE adjusts some of the parameter values and then sets up the arrays used in the mass diffusion computations. MAIN next calls WRITE_ELEV_DATA to record initial elevations. After that, MAIN counts time steps in a DO loop, calling subroutines to compute drainage, sediment transport, and uplift for each time step.

Within the time loop, MAIN first calls the subroutine RESET_VARIABLES to reset certain variables back to zero for a new time step. Next, it calls subroutine FIND_NEXT_NODE. This subroutine identifies the direction of steepest downward slope at a given cell and records the coordinates of the adjacent or neighbor cell in the NBRX( ) and NBRY( ) arrays, and the slope in the SLOPE( ) array. Next, subroutine DRAIN_BASIN calculates the drainage of closed basins (lakes). To do this, it uses an iterative algorithm that maintains a list of all cells that are in the flooded region. During each iteration, the lowest cell along the perimeter of the flooded region is identified. If this cell can drain downwards into a cell that is not part of the flooded region (but which can be part of a previously calculated lake), that cell is flagged as the outlet for the lake. If not, then the cell is added to the list and the process is repeated. Boundary cells are always considered to be outlets.

MAIN next calls subroutine STREAM_TRACE, which calculates the discharge at each cell by tracing the route of each incoming "parcel" of precipitation

until that parcel flows into a boundary cell. Whether this flow is channelized depends upon a call to subroutine CHANNEL_INIT, which tests for the initiation of channels based on a threshold function of slope and discharge. Channels are defined to exist wherever this function exceeds a given threshold value. Elsewhere, cells are considered to be hillslopes and subject only to hillslope processes. Channels are therefore not permanent, but can appear and disappear as tectonics and stream piracy alter the drainage network.

Once the channels have been defined, elevation changes due to hillslope processes are computed in subroutine HILLSLOPE, which calculates the diffusion of mass in two dimensions using the ADI method. The boundaries are configured to represent a landscape surface that slopes downward to the west, striking north-south. The west boundary ($x = 0$) is pinned at its initial value. The east boundary follows the adjacent column of cells. For the north and south boundaries, a three-cell gradient is maintained such that $dh/dy = 0$. This introduces a small amount of inaccuracy near these boundaries. This subroutine can be easily modified to pin the east boundary as well, so as to simulate a rising orogen that strikes north-south and is bounded on the east and west by regions of fixed elevation.

Next MAIN calls subroutine FLUVIAL to compute sediment transport rates in the channels and elevation changes in them due to spatial gradients in the rates. The carrying capacity of a stream segment is proportional to local stream power. In general, some of the transport capacity will be taken up by sediment passed from upstream. For this reason, cells must be processed in upstream-to-downstream order (accomplished using the subroutine SORT_BY_ORDER). FLUVIAL uses the BISECT function to find an elevation change DH such that the resultant stream power is exactly sufficient to transport the resulting sediment load (this method is more stable than computing stream power based on the initial, rather than the final, slope). Two values, LOW and HIGH, must be supplied as the bounds for the bisection algorithm. They represent the cases of maximum erosion and maximum deposition, respectively. Once DH has been found, the new sediment load at the cell is added to the sediment load of the downstream cell.

Flooded cells are treated as follows: the sediment load passed to each flooded cell is deposited in that cell, up to just above the water level (which is defined by

the elevation of the outlet cell). Any excess sediment is then passed directly to the outlet cell. This treatment is considered reasonable as long as flooded areas and sediment loads are small. After sediment has been routed down all channels, elevations and information concerning the drainage net are written to files.

Finally, MAIN calls subroutine UPLIFT to simulate uplift by incrementing the elevation of all cells according to one of two functions mentioned previously. The time step is advanced and the cycle is repeated.

Model Input and Output

GOLEM relies on two input files, one containing process rate, threshold coefficients, and other information, and the other containing the initial elevation of each cell. The primary output file contains (1) the grid dimensions, (2) the grid spacing, (3) the elevation of each cell at each time step, (4) the channel/hillslope status of each cell at each time step, and (4) the coordinates for each neighbor cell at each time step ("neighbor" refers to the adjacent cell that lies in the direction of steepest slope). Other output files contain data on sediment yield and denudation rates.

Experiment 3-1: Drainage Net Development a la Schumm

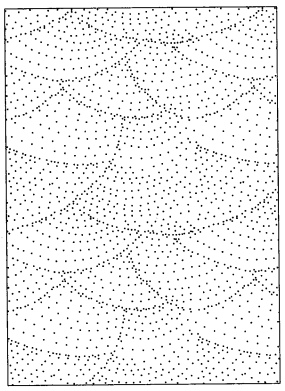

Earlier, we mentioned the sandbox experiments of Schumm and students dealing with the evolution of drainage systems. Their results provide an attractive dataset for testing GOLEM. In one of the sandbox experiments, the initial surface was graded into two intersecting planes sloping towards the outlet. Baselevel was lowered 22 cm at the start and then precipitation was applied for five two-hour periods. At the end of each period the drainage net was mapped (Figure 3-2). Results show that the drainage network slowly extended headward or elongated over the initial surface, similar to natural networks. Concurrently, the network elaborated as tributaries were added to the initial low-order streams.

A more quantifiable measure of drainage net development is sediment yield and its variation in time. As expected, yields are initially very high as the net is

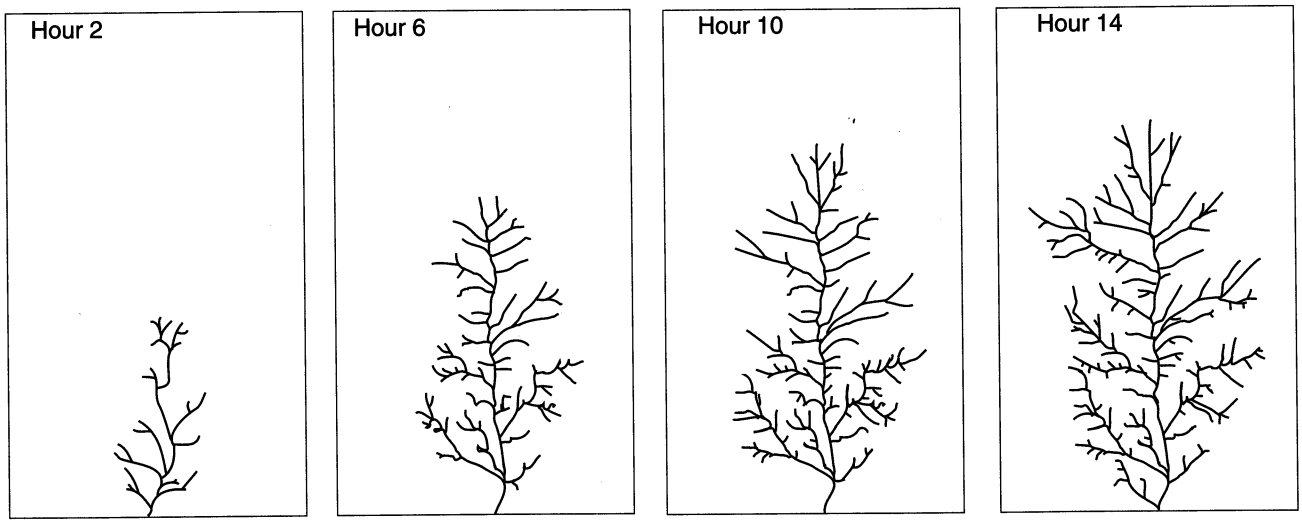

Figure 3-2 Drainage networks developed in rainfall erosion facility during Schumm and Parker's experiment E1 (Schumm *et al.*, 1987).

Table 3-1 Input data file for GOLEM, simulating sandbox experiment of Schumm.

336	/number of time steps
150	/delta t (s)
400.0	/fluvial transport coefficient
1.6	/exponent on discharge in fluvial transport equation
1.8	/exponent on bed slope in fluvial transport equation
0.0	/hillslope diffusivity
0.0	/threshold for channel initiation
1.0	/coefficient in channel initiation function
1.0	/exponent on discharge in channel initiation function
0.0	/exponent on slope in channel initiation function
0.066	/precipitation rate (m/hr)
0.0	/uplift rate (m/yr)
0	/uplift duration (timesteps)
1	/uplift type
0	/fault location (column number)
48	/output interval (timesteps)
park1.topo	/initial topography file
parker1-9	/root name of output files
1	/east boundary condition (1 = floating boundary)
0	/north and south boundary condition (0 = floating boundary)
16	/row number at which notch begins on western boundary
28	/row number at which notch ends on western boundary

carved out and a wave of dissection migrates up slope (Figure 3-3). As the net becomes established, yields decay exponentially until at the time of maximum extension, yields are 10 percent of the initial rate (Schumm et al., 1987). The initial and boundary conditions for GOLEM that simulate this experiment are listed in Table 3-1.

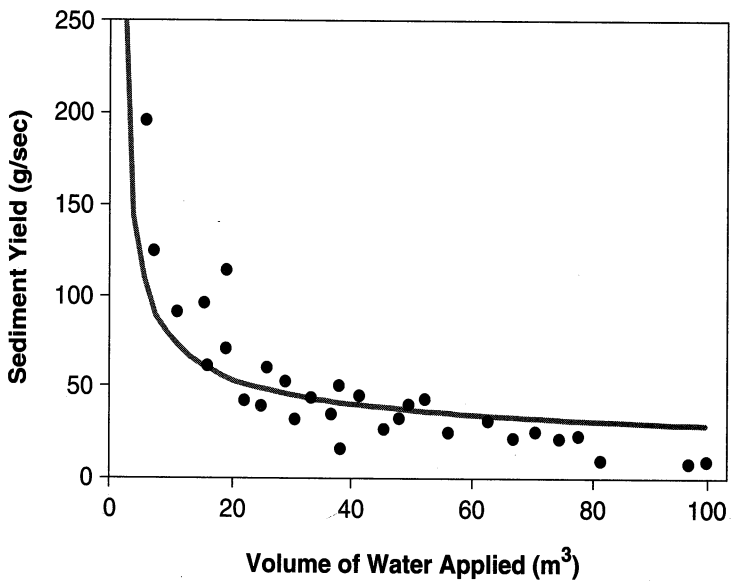

Figure 3-3 Sediment yield as function of time (expressed as volume of water applied to the rainfall erosion facility) for Schumm and Parker's experiment E1. Points represent observations by Schumm *et al.*, (1987); curved line represents results of numerical Experiment 3-1.

Results of Experiment 3-1 (Plate 3-1) show that as time progresses, the landscape is reduced in elevation and the drainage net extends headward and then consolidates, much as in Schumm and Parker's sandbox experiment. Sediment yields also decrease exponentially (Figure 3-3), although the magnitudes do not match the sandbox experiment exactly.

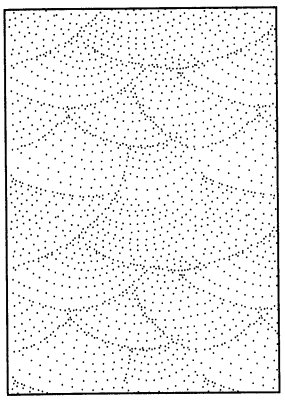

Experiment 3-2: Landscape Evolution Along the Wasatch Fault

Basin and range provinces consist of longitudinal, asymmetric ridges and broad intervening valleys formed by tilted fault blocks. The Wasatch mountains and adjacent basin in north-central Utah (Figure 3-4) provide a good example. Experiment 3-2 (Table 3-2) simulates the evolving topography of such a tilting block. The initial condition consists of a plane that slopes at 0.003 on which is superimposed 'white noise' consisting of random variations in elevation with a maximum amplitude of 20 meters (Plate 3-2).

Table 3-2
Input data file for Experiment 3-2, simulating the evolving topography of a tilting block.

```
/(See Table 3-1
for variable definitions)

100
100
0.5
0.1
0.0
1.0
1.0
0.0
0.250
1.0
20
3
21
500.0
25
w1.topo
wasatch1
0
1
0
62

Comments:
Input file for LEM
Wasatch example.
```

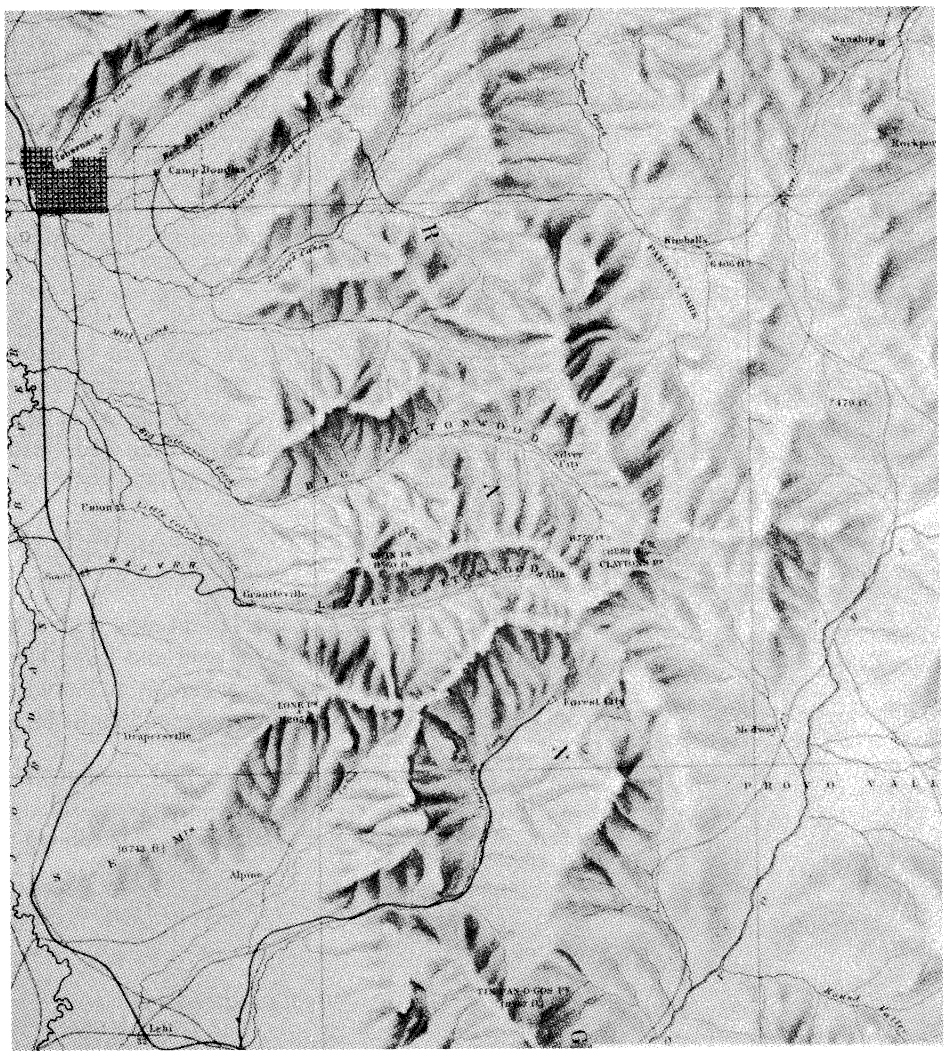

Figure 3-4
Shaded relief map from the 1870s of the Wasatch Range east of Salt Lake City, Utah. Latitude and longitude lines are spaced 15′ apart.

Results of Experiment 3-2 show that the drainage is initially ponded and deranged but through time the network becomes integrated (Plate 3-2). The drainage divide retreats back from the scarp as streams flowing down the scarp capture the headwaters of less energetic dip slope streams. Faceted spurs develop and alluvial fans grow in front of the scarp, producing topography similar to that actually observed.

AN EMPIRICAL APPROACH

Sometimes a modeling project may not warrant the detailed treatment of a landscape provided above. Alternatively, denudation of the landscape can be estimated from empirical relationships. Consider a single-thread river flowing in a two-dimensional vertical plane from a source terrain to a sedimentary basin. As shown in Chapter 4, a river of this simplicity can be represented as gradually varying, open-channel flow that erodes sediment from its bed, transports that sediment plus sediment fed into the channel from its sides, and deposits sediment back to its bed, all contingent upon the capacity and competency of the flow. The river catchment area, which extends out of the plane of the river, provides the water and sediment.

Our task here is to specify two functions, $q(x,t)$ and $qs(x,t)$, that describe the input of water and sediment to the open channel per unit length, where x is distance downstream and t is time. These functions should provide water and sediment at rates sufficient to reproduce observed increases of water and sediment discharges with increasing distance downstream in typical trunk streams. Also, we expect these functions to depend upon variables such as local relief and mean annual precipitation in the watershed. Water discharge is considered first.

Water Discharge

What is the volume per unit time per unit of downstream length $q(x,t)$ at which water enters a typical stream? The theoretical answer is simple. If rainfall is uniform at a constant rate p over a catchment of area $A(x)$, and all of the rainfall enters the stream by overland flow, then over distance x, measured downstream from the drainage divide, the volume is:

$$q(x,t) = p\frac{A(x)}{x} \qquad \textbf{(3-15)}$$

Consider a rectangular catchment area with a trunk stream running along the long axis that is fed by uniform overland flow. The drainage area $A(x)$, upstream of any point x, is given by Wx, where W is the width of the rectangle. Therefore, from (3-15), $q(x,t)$ is a constant independent of location and equal to pW.

How does this compare with actual streams? Data for q are not readily available, but values of $Q(x,t)$, the total river discharge at various locations downstream, are well known. By definition, Q is related to q as:

$$Q(x,t) = \int_0^x q(x,t)\,dx \qquad \textbf{(3-16)}$$

Therefore, in the theoretical basin:

$$Q(x,t) = \int_0^x p\frac{Wx}{x}dx = pWx = pA \qquad \textbf{(3-17)}$$

and stream discharge should be directly proportional to the area drained.

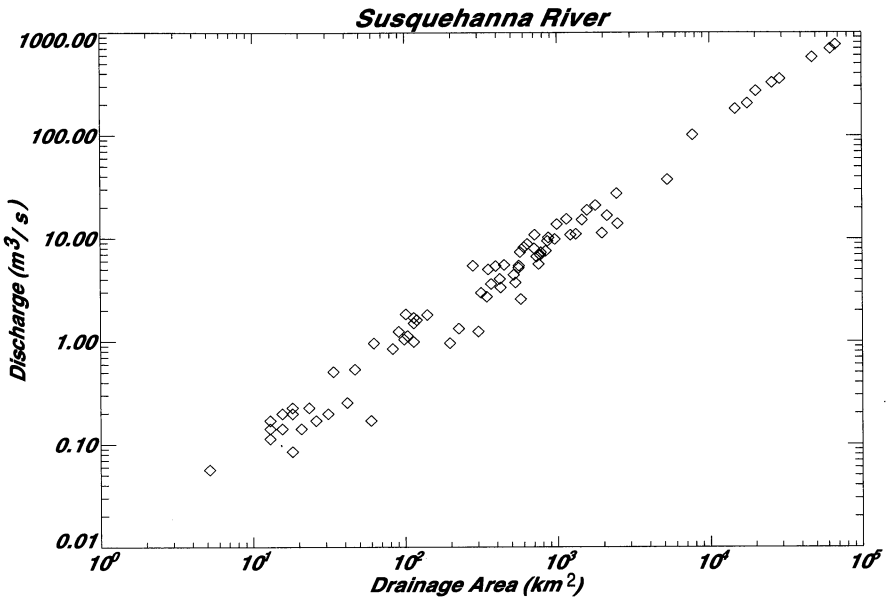

Figure 3-5
Log-log plot of water discharge versus drainage area for the Susquehanna River. Because slope of plot is about 1:1, discharge is linearly proportional to drainage area in Susquehanna River Basin of Pennsylvania (unpublished data from H. Hanson, Dickinson College, Carlisle, Pa.)

Figure 3-5 presents water discharge Q versus drainage area A for the Susquehanna River in Pennsylvania. A relationship in which Q is proportional to the first power of A on a log-log plot would consist of a line with a slope of 1. Clearly, the Susquehanna's discharge is linearly proportional to its drainage area. Unfortunately, this relationships does not hold for streams in different precipitation and geologic settings, as Figure 3-6 shows. For drainage areas up to about 1000 square kilometers, slopes of regression lines for data from Arizona and Virginia

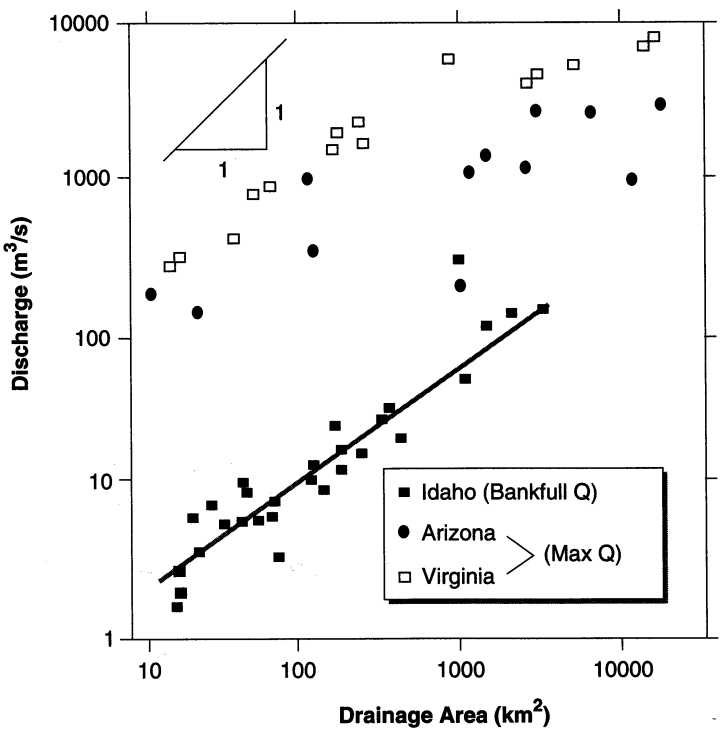

Figure 3-6
Log-log plots of water discharge versus drainage area for selected streams in Idaho, Arizona, and Virginia. Water discharge is power function of drainage area. Max Q is maximum known flood-peak discharge; bankfull Q is discharge at bankfull stage (data from Riggs, 1985, and Knighton, 1984).

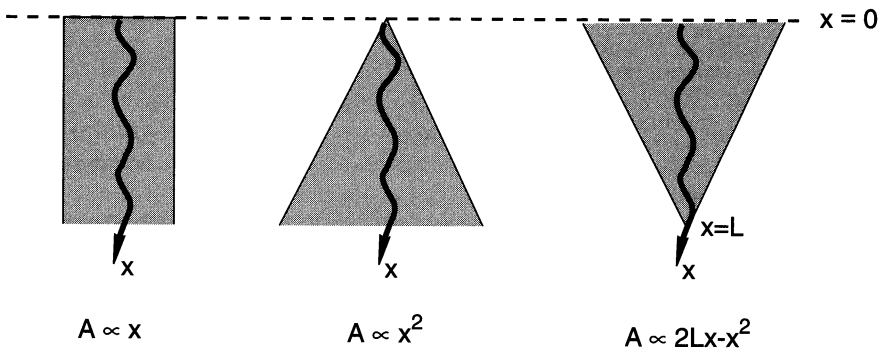

Figure 3-7 Hypothetical maps of three simple geometrical relationships between drainage area A (stippled), and distance downstream *x*. No specific scale is implied.

range from 0.9 to about 0.7. In larger drainage areas though, the Arizona and Virginia data sets yield regression line slopes of about 0.5.

These differences between our simple model and nature probably arise partly because real precipitation is not distributed evenly across catchment area and because some of the precipitation that falls in the headwaters of catchments may travel underground to appear as discharges in the river further downstream. Finally, in our simple model we assumed that drainage area is linearly proportional to distance downstream, an assumption that deserves amplification. By contrast, most textbooks in geomorphology present data from John Hack's (1957) classic study in the Appalachians, showing that drainage area varies as the 1.67 power of distance downstream. As Figure 3-7 illustrates, this means that drainage basins become wider downstream. This perplexing conclusion arises because Hack collected his data from the headwaters of drainage basins where area does increase downstream. But over whole river systems, we should expect that area will vary with distance downstream to a power ranging from less than 1.0 to 2.0.

Our simple model for $q(x,t)$ now can be revised in the light of observations. Given that:

$$q(x,t) = \frac{d}{dx}Q(x,t) \tag{3-18}$$

and,

$$Q(x,t) \propto A^m \quad and \quad A \propto x^n \tag{3-19}$$

then,

$$q(x,t) \propto mnx^{mn-1} \tag{3-20}$$

Because m ranges between 0.5 to 1 and n ranges from less than 1 to 2, again we see that $q(x,t)$ to a first approximation is independent of x.

Sediment Discharge and Denudation

In this section we present some empirical relationships between the dependent variables of sediment discharge and landscape denudation rate, and the independent variables which control them. Our objective is the same as in the previous section, because for each timestep we need to know the amount of load to remove

from a source terrain and the amount of sediment to feed into streams entering our model basin. Sediment discharge and denudation rate are used interchangeably here, although this ignores chemical denudation, the lowering of the landscape by dissolution.

While it is easy to estimate the dependence between sediment discharge and variables such as precipitation, caution is in order. The empirical functions presented here are severely limited by the data from which they have been derived. For example, sediment yields from a catchment basin are obtained by measuring the sediment load of the trunk stream and its water discharge. The accuracy of the number depends upon adequacy of the sampling equipment, sampling frequency, accuracies of stage-discharge functions, and in length of record. Often, some or all are deficient. Also, measurements of sediment load rarely include the bedload and dissolved load, thereby leaving us to guess at the total sediment discharge from a source area. This does not mean that the relationships are worthless, because many different researchers, using different methods in different areas, have obtained similar functions.

As mentioned in the previous section, the most important controls on sediment discharge and landscape denudation are local relief and climate, especially the annual precipitation and its seasonality, and mean annual temperature. These influences are treated in sequence below.

Denudation and Relief

Relief is the vertical difference in elevation between the hilltops and valleys of a region. It is often quantified as *mean local relief,* which is the mean of the differences between maximum and minimum elevation within a local area. Areas of high relief have high slopes, and because the mass flux of material on hillslopes is proportional to the first power of slope, it makes sense that the rate of landscape denudation is correlated with relief. Observations confirm this (Figure 3-8), the relationship being:

$$D_s = 0.0001535R \qquad \textbf{(3-21)}$$

where: D_s = mean denudation rate in meters per thousand years,

R = mean relief in basin in meters, with constant 0.0001535 in units per thousand years.

Some researchers correlate sediment yield with mean regional elevation (Figure 3-9), providing statistically significant correlations between relief and elevation in recent orogenic belts. For example, in Figure 3-9 the mean denudation rate D_s in km/millon years of recent orogenic belts is given by:

$$D_s = M_s/(\rho A) = 419\times10^{-3}H \qquad \textbf{(3-22)}$$

where: H = elevation in km,

M = suspended sediment load,

ρ = sediment density,

A = area of basin.

But as Summerfield (1991) has pointed out, the geologically old high plateau of southern Africa at 2 km elevation produces extremely low sediment yields because the relief is low.

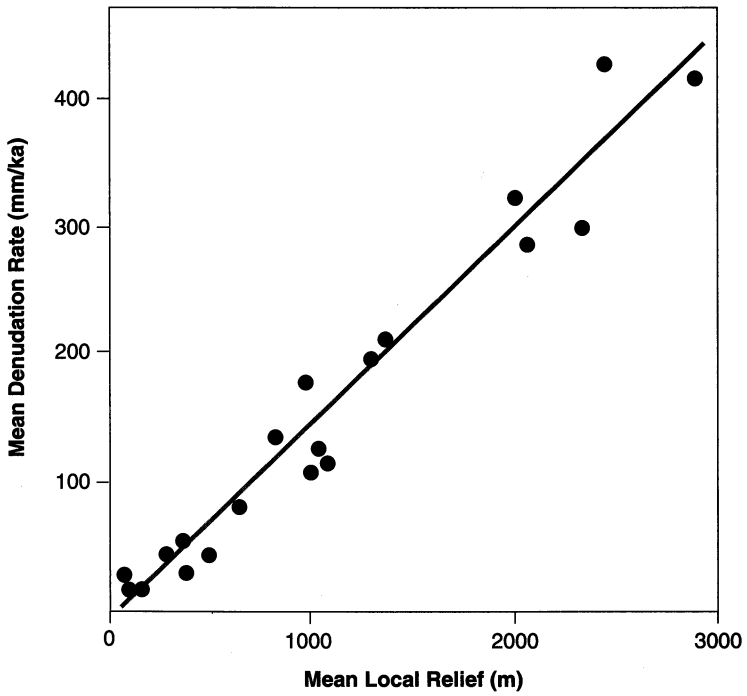

Figure 3-8 Plot of mean denudation rate (in millimeters per thousand years) versus mean local relief (in meters) for 20 mid-latitude drainage basins (after Ahnert, 1970).

It is also possible that uplift rate is another "lurking third variable." Figure 3-10 shows that denudation rates in present-day Japan correlate with uplift rates. Generally, mean elevation also correlates with uplift rates, and pre-

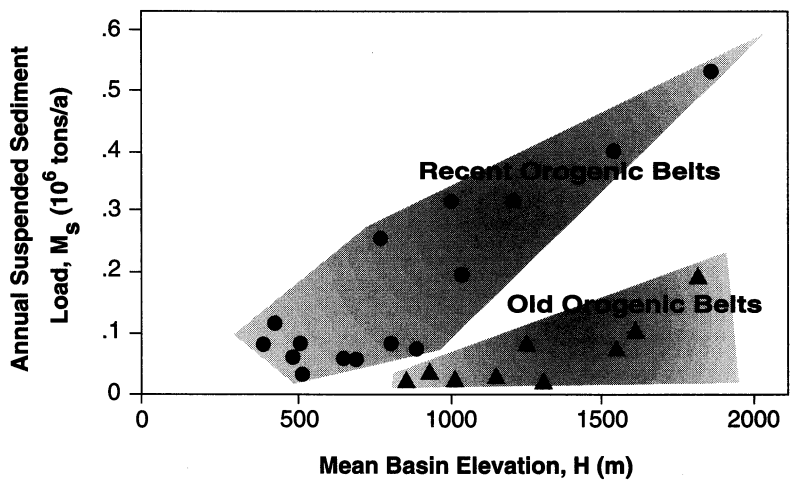

Figure 3-9 Plot of annual suspended sediment load, M_S (10^6 tons yr^{-1}) versus mean basin elevation, H(m), based on data of Pinet and Souriau (1988). Two trends are apparent if the data are segregated according to old and recent orogenic belts.

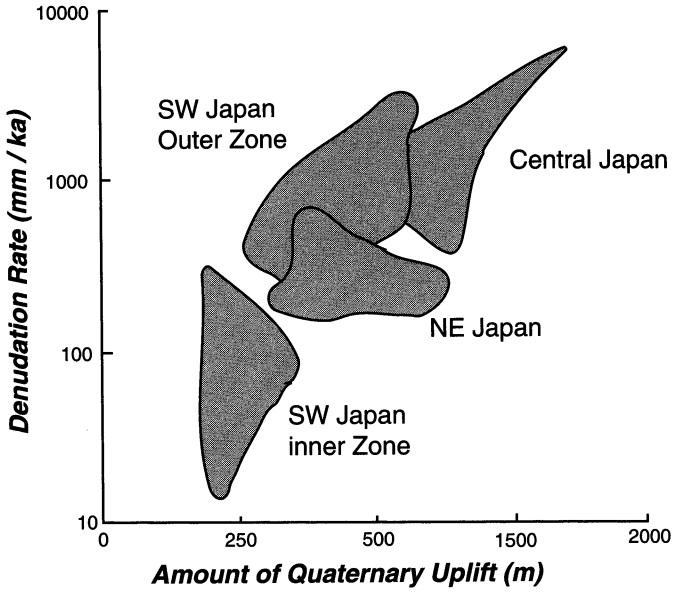

Figure 3-10
Plot of mechanical denudation rate in mm per thousand years versus amount of Quaternary uplift in meters for various regions of Japan. Inner and outer zones of southwest Japan refer to drainage basins that enter the Pacific and Japan Sea, respectively (from Yoshikawa, 1985).

cipitation sometimes correlates with mean elevation, thereby further confusing the issue. Therefore, while we will use (3-22) in some models, let the reader beware.

Denudation and Climate

Climate and its associated variable, vegetation, also play a role in controlling sediment yields, although climate is probably not as important as previously thought. While suspended sediment yields are positively correlated with mean annual rainfall at many sites (Figure 3-11 and Figure 3-12), the correlation may be misleading. On the South Island of New Zealand, for example, rainfall is orographic and strongly correlated with elevation there and therefore with relief. But it is not clear how much of the variance in sediment yield (Figure 3-11) is due to precipitation and how much is due to steep local slopes. Nevertheless, when data are combined over a wide range of precipitation values (Figure 3-13), plots yield lines or curves similar to those in Figure 3-11 and Figure 3-12. Denudation rate increases with precipitation up to about 400 mm mean annual precipitation, whereupon the effects of vegetative cover outweigh increased runoff and denudation rate decreases. Eventually, with increasing precipitation, increasing runoff overwhelms the protective effect of vegetation and denudation rates rise again.

Older textbooks asserted that climate plays the dominant role in landscape denudation. In fact, recent data (Summerfield, 1991) show that denudation rates vary by an order of magnitude between lowlands and adjacent mountains, whereas in mountainous terrains in different climatic and vegetative zones, denudation rates vary by a factor of 5 to 9. Thus, the role of climate in denudation may be less than relief.

The relationship between chemical denudation and precipitation (here measured as runoff), while not showing the two maxima of Figure 3-13, also involves a positive correlation (Figure 3-14). Unlike physical denudation, chemical denudation is only weakly related to elevation or relief. Further, the role of basin lithology also is weak at best. In summary, it appears that local relief dominates

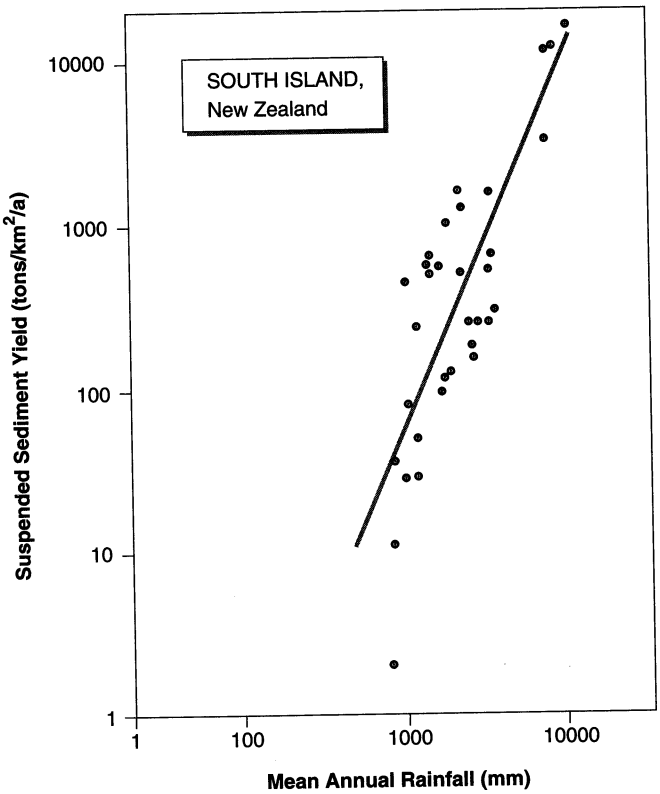

Figure 3-11
Log-log plot of suspended sediment yield versus mean annual precipitation for South Island of New Zealand. Suspended sediment yield is positively correlated with mean annual precipitation (from Walling and Webb, 1983).

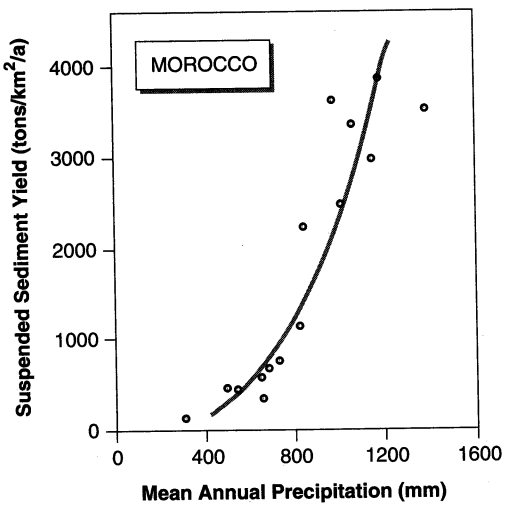

Figure 3-12 Plot of suspended sediment yield versus mean annual precipitation for Morocco showing positive correlation from Walling and Webb (1983).

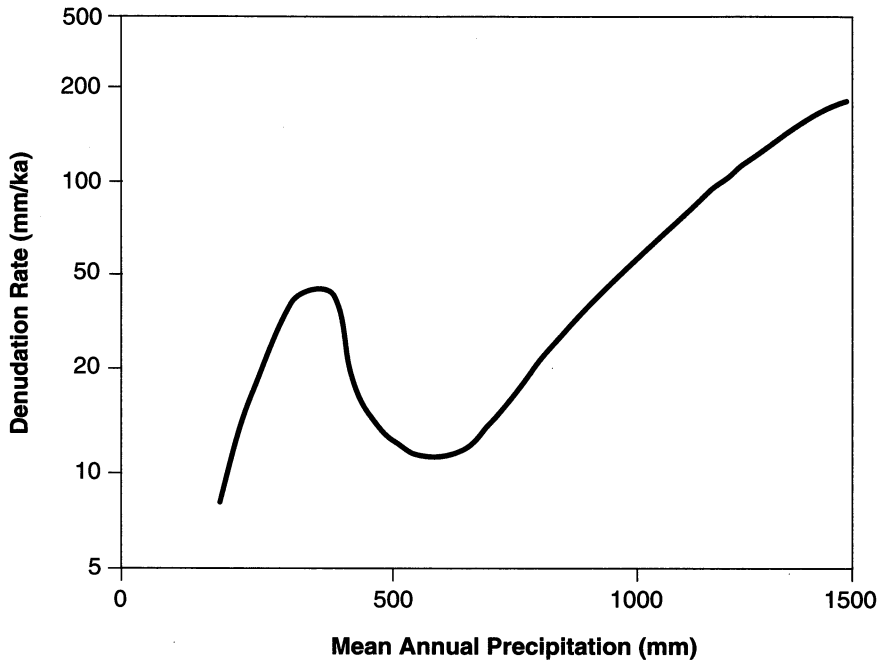

Figure 3-13 Plot of mechanical denudation rate versus mean annual precipitation showing two maxima (Ohmori, 1983).

denudation rates of today's landscapes and, although lithology and soil type may be locally important, they will not be considered further here.

It remains for us to define the rate of addition of sediment to a stream per unit stream length, $q_s(x,t)$, consistent with these observations. As with water discharge

$$q_s(x,t) = \frac{d}{dx}Q_s(x,t) \qquad \textbf{(3-23)}$$

where: Q_s= suspended and bedload sediment discharge rate.

By definition, $Q_s = D_s A$, where D_s is the mean denudation rate and A is drainage basin area, and therefore, by (3-19) and (3-21):

$$Q_s(x,t) \propto RA \propto Rx^n \qquad \textbf{(3-24)}$$

Therefore substituting (3-24) into (3-23), and assuming relief does not depend upon x, yields:

$$q_s(x,t) \propto nRx^{n-1} \qquad \textbf{(3-25)}$$

Because n ranges between a number less than 1 and 2, $q_s(x,t)$ to a first approximation is either independent of x, or linearly dependent upon x.

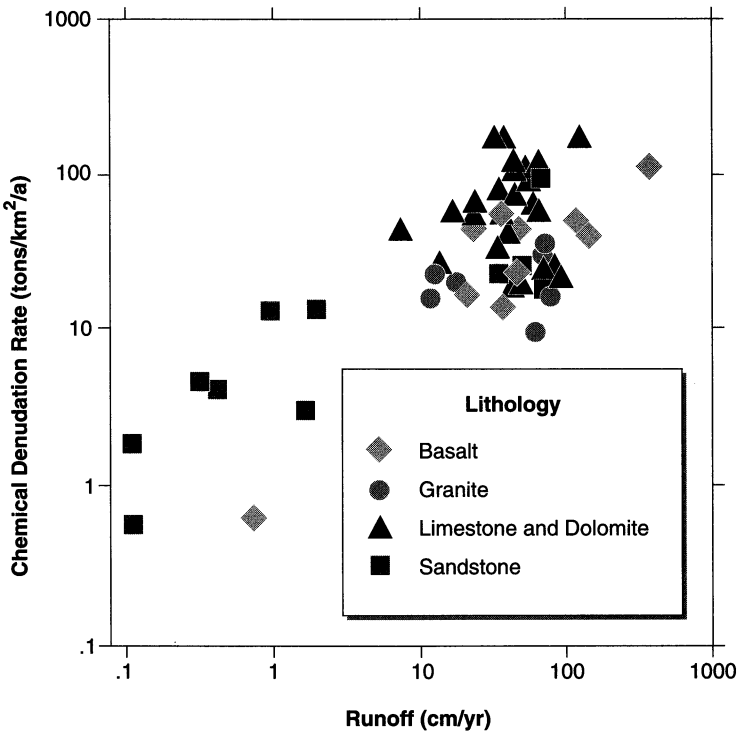

Figure 3-14 Log-log plot of chemical denudation rate measured as mean annual dissolved load of rivers, versus mean annual runoff. Chemical denudation rate is positively correlated with mean annual runoff. Vertical spread in dissolved load for given runoff is due to varying lithology in drainage basin. Drainage basins underlain predominately by volcanic or carbonate rocks chemically denude faster than basins underlain by granite (after Walling and Webb, 1986).

PREDICTING GRAIN SIZE DISTRIBUTION OF SEDIMENT FEED

Now that we have some indication of the amount of sediment that a source terrain can yield, we need to predict its textural properties. Generalizations are not possible at our present state of knowledge, but we can offer a specific example thanks to Ibbeken and Schleyer (1991) of the Freie Universität Berlin. They recently summarized twenty years of provenance studies involving nineteen small rivers draining Calabria at the southern tip of Italy. They chose Calabria because it is in an active plate tectonic setting and experienced uplift of over 1 km in the Pleistocene. A Mid-Pleistocene erosion surface allows the calculation of erosion rates over an area of 2000 km^2. The relief is high such that steep slopes create landslides. The rock types are equally divided among granite, metamorphic, and sedimentary. Mean precipitation ranges from less than 600 mm/yr at the coast to greater than 2000 mm/yr in the central mountains. Finally, man's impact is low.

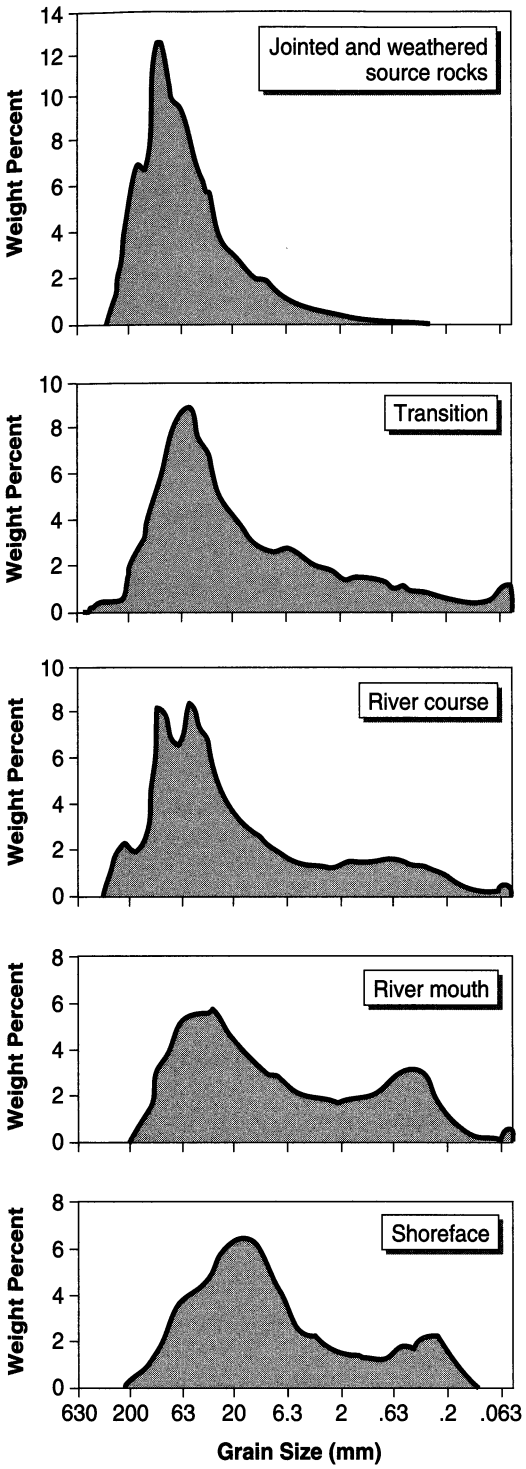

Ibbeken, Schleyer, and colleagues sampled five sedimentary environments from source to basin as follows: (1) jointed and weathered source rocks in situ, (2) transition environments including regolith, talus, and alluvial cones, (3) river course environments downstream of the fall line, (4) river mouth environments, and (5) beach or shoreface environments. Figure 3-15 shows histograms of grain sizes from these environments. Along the transport path from jointed and weathered in situ source rocks to regolith and shoreface, the grain size distributions pass from a unimodal Rosin distribution, characteristic of rocks crushed in a breaker mill, to a bimodal Gaussian distribution, characteristic of water-laid sediments. The mean of the coarser mode in the bimodal distributions decreases from 64 mm to 21 mm. Although not shown here, the jointed and weathered source rocks show roughly similar distributions, whether they are sandstones, limestones, or granites. The causes of the shift in grain sizes are principally comminution and selective sorting, as discussed in Chapter 4. The point here is that the size distribution of the samples from transition environments is a first approximation of the sizes delivered to a fluvial system in an orogenic source terrain.

Figure 3-15
Aggregate histograms of grain size distributions in five sedimentary environments of Calabria, southern Italy. See text for details. From Ibbeken and Schleyer (1991, Fig. 10.2).